

Accepted Manuscript

A new test method for investigating punching shear strength in Ultra High Performance Fibre Reinforced Concrete (UHPFRC) slabs

A.M.T. Hassan, G.H. Mahmud, S.W. Jones, C. Whitford

PII: S0263-8223(15)00508-5

DOI: <http://dx.doi.org/10.1016/j.compstruct.2015.06.044>

Reference: COST 6543

To appear in: *Composite Structures*



Please cite this article as: Hassan, A.M.T., Mahmud, G.H., Jones, S.W., Whitford, C., A new test method for investigating punching shear strength in Ultra High Performance Fibre Reinforced Concrete (UHPFRC) slabs, *Composite Structures* (2015), doi: <http://dx.doi.org/10.1016/j.compstruct.2015.06.044>

This is a PDF file of an unedited manuscript that has been accepted for publication. As a service to our customers we are providing this early version of the manuscript. The manuscript will undergo copyediting, typesetting, and review of the resulting proof before it is published in its final form. Please note that during the production process errors may be discovered which could affect the content, and all legal disclaimers that apply to the journal pertain.

A new test method for investigating punching shear strength in Ultra High Performance Fibre Reinforced Concrete (UHPFRC) slabs

A.M.T. Hassan^a, G.H. Mahmud^b, S.W. Jones^b, C. Whitford^b.

^a Department of Civil Engineering, Architecture and Building, Coventry University,
Coventry CV1 3FP, UK

^b School of Engineering, University of Liverpool, Liverpool L69 3GQ, UK

Abstract

Punching shear capacity of Ultra High Performance Fibre Reinforced Concrete (UHPFRC) slabs has been the subject of a number of studies. There is, however, only limited information available on this parameter of UHPFRC without conventional reinforcement. This is due to the complexity of punching shear behaviour within concrete and is also limited by the lack of suitable test methods currently available. Therefore, in this study, attempts to design a novel testing method to measure the punching shear capacity of the concrete was carried out. The designed test arrangement was employed to carry out an extensive experimental study on UHPFRC slabs subjected to punching shear failure. From the results obtained, the relationship between the punching shear load and the angle of the shear plane, the critical value of the basic control perimeter and failure mode were studied. The experimental study undertaken here provides significant insight into the punching shear capacity of UHPFRC slabs. The results illustrate and highlight many of the advantages of using UHPFRC compared to normal concrete in structural designs. The novel punching shear test presented here has established itself as a suitable procedure for testing UHPFRC and potentially, other fibre reinforced composites.

Keywords: Punching shear load and angle, Basic control perimeter, Punching shear failure behaviour, UHPFRC.

Corresponding author. Tel: 02476887950
E-mail address: aram.hassan@coventry.ac.uk (A.M.T. Hassan)

1. Introduction

The high tensile and compressive properties of UHPFRC have been well reported [1-4]. The improved properties of this concrete has allowed structural members to be built with complex forms, lower volume of conventional steel reinforcement or maybe none, and lower maintenance costs. The improved tensile behaviour of UHPFRC can be exploited to enhance the shear resistance of its structural members, particularly in highway bridge applications.

Structural failures of highway bridge structures are not common under static loading. However, in highway bridges, beam and slab failure usually occur in two common forms, direct flexural and/or punching shear. The direct flexural failure typically occurs in beam or slab members and is associated with overall bending. This type of failure arises from the formation of diagonal tension cracks in the region of maximum bending moment and extends across the entire width of the member. However, punching shear failure is a more localised effect associated with thin slabs or two-way slab-column members when subjected to a highly concentrated load. Punching shear failure occurs when the principal stress across the critical surface of the section exceeds the tensile strength of the concrete due to applied loading and failure occurs with limited warning. An example of this type of complete failure is seen in Figure 1. Failure occurs with the potential diagonal crack following the surface of a truncated cone around the load. The failure surface extends from the bottom of the member diagonally upward to the top surface. For a normal concrete slab, the angle of inclination of the failure surface ranges approximately from 20 to 45 degrees depending on the amount of shear reinforcement [5]. However, very little information on this parameter is available for UHPFRC.

The actual behaviour of concrete members in shear is complex and difficult to analyse theoretically. Shear failure usually results from a combination of shearing forces and bending moments. The current codes of practise such as Eurocodes and ACI have proposed reasonably simplified procedures for the analysis and design of conventional concrete members for punching shear resistance. These guidelines are based on results from many experimental investigations [6]. However, these design equations have limitations and not suitable when it comes to UHPFRC. The design equations do not fully take into account the increase in the punching shear capacity of UHPFRC given the improved compressive and/or tensile strengths associated with the concrete.

Since becoming commercially available, ultra high performance fibre reinforced concrete has been used in construction under many different commercial names such as Ductal®, compact reinforced composite, reactive powder concrete, and ultra-high performance concrete (UHPC) [7-11]. In the last few years, UHPFRC has become popular in construction and a number of optimised UHPFRC sections have been proposed for highway bridge applications, see Figure 2.

Such bridge girders appear to have been optimised to the limit. However, knowledge of the structural behaviour of these girders, in particular, the shear strength without steel reinforcement is very limited. So far, punching shear capacity of UHPFRC has been the

subject of a number of studies [12-14]. However, difficulties in determining this property have been reported due to the occurrence of flexural failure prior to punching shear during testing [12-14]. Therefore, specific knowledge of the shear strength in isolation from the effects of flexural damage is required to contribute towards the design of UHPFRC in construction. However, very little information is available on this property due to the complexity of punching shear behaviour of UHPFRC and also due to lack of a suitable testing methodology. Therefore, in this study, a novel testing method has been designed to accurately measure the punching shear behaviour of UHPFRC. Detailed experimental investigations on the punching shear behaviour of UHPFRC slabs without steel reinforcement subjected to high concentrated load were carried out. Various parameters ranging from the relationship between punching shear load (V_{nd}) and angle (θ), the critical value of the basic control perimeter (u) to the failure mode were investigated.

2. Experimental studies

In this study, a series of cube and slab specimens were cast and tested. The cube specimens were tested to obtain density and compressive strength measurements at 28 days. The slab specimens were also tested at 28 days to obtain punching shear behaviour. In this section, the development of the punching shear test method and the experimental study are presented. This include, test development, mix composition, specimen preparation and test setup arrangements.

2.1 Test Development

A number of trial tests were conducted to characterise the punching shear capacity of the concrete with minimum influence of bending stress. The trial tests were performed and modified throughout the experimental program until the final test setup was developed. It must be noted that there are no existing standards for measuring the punching shear capacity of UHPFRC slabs or the test method described here. The experimental investigation was divided into three phases, as discussed below.

In the first phase, preliminary tests were carried out on rectangular slabs of 300x300x30 mm in length, width and depth, respectively. The size of the specimens was kept small due to the high cost of the material. However, large enough so that punching shear failure could occur during testing. The specimens were supported on two different boundary conditions, simply supported on four edges and circular hollow steel rings with various diameters. The load was applied to the centre of the specimen using a 50 mm diameter steel indenter. The small loaded area was used to enhance the possibilities of punching shear failure. From the results obtained in this phase, it was observed that the influence of flexural failure was not only present but quite significant. The flexural failure was far more pronounced in the simply supported specimens as opposed to those with circular supports. A combination of flexural and shear failure was observed from the results of this phase.

In the literature, fixed boundary conditions was reported to improve the possibility of punching shear failure of thin UHPFRC slabs [12, 13]. This is due to the reduction of the

maximum bending moment in the region of punching shear. However, the influence of flexural stress was still reported to be significant. Therefore, this study took a different approach to develop a test setup that can minimise the effect of flexural failure on punching shear tests.

The second phase was to increase the thickness of the slab specimens to 60 mm and incorporate an initial notch, similar to notched beam specimens in bending tests. Circular notches of 30 mm depth of different diameters were introduced at the centre of the specimens, as shown in Figure 3. There were two purposes to this design: 1. to provide a notch which initiates a shear plane along a predefined path and cause punching failure; 2. provide increased flexural stiffness in the slab. Various notch diameters from the inside edge of the notches ranging from 55.5 mm to 162 mm were introduced which provided a wide range of punching shear angles relative to the applied load. In this phase, the circular boundary condition was used.

This method forced the failure of the slabs at the notch positions. Results obtained in this phase appeared to be promising, but inconsistent. The influence of flexural and hoop stresses were present, and so an improvement in the test setup was required. Figure 3, provides a schematic indicating the test setup at this stage.

In the third and final phase, the flexural and hoop stress effects were reduced significantly. This was achieved by increasing the depth of the shear notches and using an improved supporting arrangement. The specimen's total thickness was increased from 60 mm to 90 mm. The initial notch depth was increased from 30 mm to 60 mm and the effective slab thickness was kept at 30 mm. The depth of the notches was increased to minimise flexural stress before the occurrence of punching shear failure. In addition, the specimens were supported close to the perimeter of their notches using circular steel tubes of various diameters. The inside diameter of each support was equal or smaller than 1.30 times the diameter of the notch. The various sizes of circular boundary condition was used to minimise warping and hoop stress as had been encountered in the preliminary stages of the tests. The results obtained from this phase were predominately punching shear failure and the objective of the investigations was achieved as demonstrated in the results and discussion section. The final test setup is shown in Figure 4.

2.2 UHPFRC mix

The mix proportion adopted in this study is summarised in Table 1 [15]. In the mix, Portland cement (CEM 1) with a strength class 52.5 N was used. Two types of supplementary cementitious materials were used; ground granulated blast-furnace slag (GGBS) and silica fume (SF) supplied by Appleby Group Ltd and Elkem Materials, respectively.

The chemical, physical and mechanical properties of the cement, GGBS and SF used in the mix can be found elsewhere [3]. The aggregate, silica sand was supplied by WBB Minerals UK, with an average particle size of 270 microns. A polycarboxylate-based superplasticiser

known as Structuro 11180 was supplied by FOSROC Ltd. The steel fibres were straight high carbon steel with a tensile strength of 2000 MPa, 13 mm in length and 0.20 mm in diameter, supplied by Bekaert Ltd.

For the mixing process, materials were weighed and placed in a horizontal pan mixer in the order: silica fume, cement, GGBS, and silica sand. The materials were firstly dry mixed for 5 minutes before water and superplasticiser were added. The materials were mixed for a further 10 minutes until the dry powder mix transformed into a wet paste concrete. At this stage, steel fibres were slowly added by hand to the wet concrete paste in the mixer. The concrete was mixed for a further 2 minutes to ensure proper dispersion of fibres in the mix after which the specimens were cast. The specimens were compacted on a vibrating table for nearly 1 minute. After compaction, all the specimens were covered with damp hessian and polythene sheets, and kept at laboratory temperature (approximately 20 °C) for 24 h. In total, 22 rectangular slabs and 9 cube specimens were cast. Once initial setting has occurred, demoulding took place at approximately 24 h. All the specimens were submersed in a curing tank in an elevated temperature of 90°C for the next 48 h and finally kept at laboratory temperature until testing.

2.3 Specimen preparations

In the third phase, the dimensions of the slab specimens were 300x300x90 mm in length, width and depth, respectively. The cube specimens were the standard size of 100 mm.

Prior to introducing the shear notches, the trowel side of the slab specimens were ground to provide an even surface for notching, as shown in Figure 5. Soon after grinding, a mechanically secured pillar drill with diamond core bits of various diameters were used to introduce the shear notches to the underside of each specimen in the centre, as shown in Figure 6. The width of the notches was approximately 4 mm to 4.5 mm. Table 2 summarises the notch diameters, support diameters and thickness, basic control perimeter and the punching shear angles of the specimens.

2.4 Test setup

The specimens were tested using a 300 kN Zwick testing machine. The load was applied at the centre and opposite side to the notches using a 50 mm diameter steel indenter. The test was conducted under displacement control at a rate of 0.1mm/min up until a vertical deflection (δ_{rd}) of 9.5 mm was recorded. For deflection measurements, an LVDT was positioned under the specimen in line with the centre of the load indenter. For each notch size, three or more specimens were tested and punching shear load against deflection data was acquired digitally. Figure 7 shows the test setup in the testing rig.

After each test, the failed specimen was removed from the testing rig and checked visually to investigate any signs of flexural failure. Finally, the specimen was placed back into the loading rig and reloaded again to cause total failure. In this way, the punching shear cone of

the specimen was forced through and investigations on the modes of failure and fibre distribution in the concrete were carried out.

3. Results and Discussion

3.1 Load vs deflection

The mean compressive strength and density of the concrete at 28 days were 166.2 MPa and 2450 kg/m³, respectively. The test results for the slab specimens presented here were obtained from the developed test method (final phase) described in Section 2.3. The full test results of this phase is summarised in Table 3.

At the beginning of each test, concrete crushing was observed, in particular, for slab specimens with the smallest notch diameters (55.5 and 81.5 mm) as they were exhibiting higher punching shear loads. The loads versus vertical deflections for both test results are presented in Figures 8 and 9, respectively. In both figures, concrete crushing is apparent as the initial elastic stiffness of the test results experience a dip in the beginning of each test, however, this seemed to be insignificant on the final test results.

In Figure 8, the load increases in a linear rate until the maximum punching shear load is achieved and failure occurs with limited warning. This finding is consistent with typical punching shear failure for normal concrete. Specimens with a perimeter distance of 0.53d (Figure 9) experienced crack formation before the maximum load was reached and one ductile failure was also reported. The load-deflection response indicates failure of the matrix before the peak strength was reached and fibre contribution starts just before total failure. Five out of the six tested specimens failed in a brittle manner, hence failure mode was considered brittle.

The load versus vertical deflections for the remaining specimens with basic perimeter distances of 1.02, 1.38, 1.62 and 1.87d are presented in Figures 10 to 13, respectively. In all these figures, the load increases in a linear manner until approximately 90% of the maximum punching shear load. Subsequently, strain hardening occurs for a short period until the maximum load is reached. In these tests, the specimens were able to sustain reducing load after their peak strength and continued to deform in a ductile manner, similar to a typical UHPFRC flexural failure [4].

3.2 Punching shear load vs angle

Figure 14 provides the relationship between the punching shear load and the failure angle within the concrete. The ultimate punching shear load increases with greater punching shear angles. This is as expected because the greater the angle of shearing, the greater the proportion of the force that is resisted by shear strength as opposed to tensile strength. This behaviour is known as shear support enhancement. It describes that the punching shear capacity of the concrete increases with the increase of the punching shear angle due to extra enhancement from the compression struts provided by the concrete. As expected, the punching shear load is the smallest at a basic control perimeter of approximately 2d (28.2°).

3.3 Failure behaviour

The failure behaviour of specimens with perimeter distances of $0.09d$ and $0.53d$ was very similar to the punching shear failure of conventional concrete, i.e. brittle with limited warning. For UHPFRC, an improvement in ductility was expected due to the presence of steel fibres in the concrete. However, this was not seen for specimens with a basic control perimeter of $0.09d$, while little was reported for specimens of $0.53d$. The abrupt and brittle failure of these tests resulted from a number of factors, and these can be summarised as follows:

- The steep punching shear angles,
- The lack of random fibre distribution along the shear line failure, hence lack of fibre bridging effect,
- Confined shear crack patterns, and
- The high intensity of shear stress close to the loading plate.

The punching shear angles in the tests were 84.8° and 62.3° , respectively. At such steep angles, random fibre orientation along the shear plane is not likely to be achieved. In addition, the number of fibres resisting the shear load for both sets of specimens is small, relative to their small punching shear areas. It is possible that the tensile load transferred from the fibres to the concrete prior to immediate failure of the specimen is also very small. As a result, most of the steel fibres along the shear plane experienced direct shear failure with minimal fibre bridging effect, and the matrix alone was more likely to resist most of the shear load up until failure. Hence, failure occurred when diagonal tension or combined action of shear and direct stress exceed the tensile strength of the concrete and resulted in the occurrence of confined diagonal shear cracks. Another factor could be due to the high intensity of the shear stress in the region close to the loading plate (smaller basic control perimeters). The brittle failure behaviour for almost all the specimens in Figures 8 and 9 is a result of the combination of all the factors described above.

The conical punching shear failure shapes of specimens with basic control perimeters of $0.09d$ and $0.53d$ are shown in Figure 15. It is evident that failure had occurred when shear cracks have initiated and radiated outwards from the point of the applied load to the shear notches on the tension side of the specimen forming a radiated failure cone. From these cones, a mixture of failed fibres and fibre pull-out behaviour were observed, in particular, specimens with basic control perimeters of $0.09d$.

The load-deflection curves presented in Figures 10 to 13 indicate ductile failure behaviour for all the specimens tested and total failure did not happen suddenly. Deformation of approximately 0.5 mm and greater with multiple cracking occurred before maximum load was reached. This type of failure for concrete slabs without conventional reinforcement is

different to typical punching shear failure reported for normal concrete [16]. To ensure the results obtained here are actually punching shear failure, the failed specimens were examined individually. In Figure 16, the failure behaviour of some of the tested specimens is shown, and the shape of the truncated cone failure is very similar to a typical punching shear failure that has been demonstrated in the literature for normal concrete [17] and those shown in Figure 15. The stub punching of the load indenter for all the tests and the crack pattern at the loaded face over a small area with a diameter almost the same of the loading indenter are a clear indication of typical punching shear failure. From Figures 15 and 16, it is evident that the test setup has caused the occurrence of punching shear failure of all the tests. Furthermore, the punching of the load indenter through the slab and the truncated cone failure shape were observed for every tested specimen in this study. Results from this study prove that the novel punching shear test presented here is a suitable procedure for testing UHPFRC and potentially other fibre reinforced composite slabs with minimal flexural influence.

Furthermore, the variations in failure behaviour for specimens in Figures 8 and 9 to those in 10 to 13 are down to the significant differences in the punching shear angles, punching shear areas, fibre distribution, and the fibre bridging effect in each of the tests. With smaller punching shear angles and greater punching shear areas, the number of steel fibres bridging the shear crack surfaces increase in the failure region. As a result, greater fibre pull-out forces are transferred across the cracks once the maximum load is reached. Hence, the fibre bridging effect after formation of microcracks becomes more effective and results in ductile failure. The considerably improved ductile behaviour reported for specimens with a basic control perimeter of $1.02d$ and above is significant in structural design and such behaviour can be exploited for structures where punching shear failure is imminent and the option of heavy shear reinforcement is limited in the member, i.e. thin UHPFRC highway bridge decks. This ductile behaviour can be used in UHPFRC design to reduce the basic control perimeter by half ($1.02d$) compared to what has been specified in EC2 for conventional concrete ($2d$).

4. Conclusions

In this study, an extensive experimental programme was carried out to develop a novel testing method to study the punching shear behaviour of UHPFRC slabs with minimal flexural influence. Results obtained here were used to investigate the relationship between punching shear load and angle, the critical value of the basic control perimeter and the failure behaviour of the concrete under a concentrated load. The following conclusions can be drawn from the results:

- The ultimate punching shear load was found to increase with greater punching shear angle due to the extra enhancement from the compression struts in the concrete. This behaviour is known as shear support enhancement. The punching shear load was found to be the smallest at a punching shear angle of 28.2° (basic control perimeter of approximately $2d$). This is in close agreement to what has been reported for normal concrete [17].

- From the examination of the failure modes of the tests, all the slabs failed with a truncated cone shaped on the supported side and a stub punching on the loaded side. This failure mode is similar to the typical punching shear failure reported for normal concrete [6], and validates the accuracy of the test method developed in this study.
- The failure behaviour for UHPFRC slab specimens with punching shear angles equal to and greater than 62° (basic control perimeter of $0.53d$ and smaller) were found to be brittle, similar to the typical punching shear failure behaviour for normal concrete [6]. However, the failure behaviour changed to a ductile mode for specimens with punching shear angles equal to and smaller than 45° (basic control perimeter of $1.02d$ and greater), similar to its typical flexural failure reported in the literature [4].
- The improved ductility of these tests resulted from the fibre bridging effect along the shear planes in the concrete. As a result, the slab specimens could undergo greater deflection after the maximum load was attained. Such ductile behaviour is the preferred failure mechanism for slabs in concrete designs.
- The findings reported here on the punching shear failure behaviour of UHPFRC slabs with no shear reinforcement are significant. The results illustrate a reduction of the basic control perimeter for UHPFRC slabs by half compared to what is specified in EC2 for conventional concrete. This improved ductility of the concrete in punching shear failure with its high tensile strength can be exploited to limit shear reinforcement in UHPFRC slab members to $1d$ when required. This behaviour is beneficial in the design of structures where punching shear failure is imminent and the option of heavy shear reinforcement is limited in the member, i.e. thin UHPFRC highway bridge decks.

Acknowledgments

The authors gratefully acknowledge the financial support from the Engineering and Physical and Science Research Council, UK for their support of this study through a DTA award.

References

- [1] P. Richard, M.H. Cheyrezy, Reactive powder concretes with high ductility and 200 - 800 Mpa compressive strength, American Concrete Institute, 144 (1994) 507-518.
- [2] B.A. Graybeal, Characterization of the behavior of ultra-high performance concrete, University of Maryland, Maryland, United States, 2005, pp. 360.
- [3] S.L. Yang, S.G. Millard, M.N. Soutsos, S.J. Barnett, T.T. Le, Influence of aggregate and curing regime on the mechanical properties of ultra-high performance fibre reinforced concrete (UHPFRC), Construction and Building Materials, 23 (2009) 2291-2298.
- [4] G.H. Mahmud, Z. Yang, A.M.T. Hassan, Experimental and numerical studies of size effects of Ultra High Performance Steel Fibre Reinforced Concrete (UHPFRC) beams, Construction and Building Materials, 48 (2013) 1027-1034.
- [5] A.H. Nilson, D. Darwin, C.W. Dolan, Design of concrete structures, McGraw Hill, 13th Edition 2003.
- [6] W.H. Mosley, R. Hulse, J.H. Bungey, Reinforced concrete design to Eurocode 2, Palgrave MacMillan. 7th Edition 2012.
- [7] M. Andrade, M. Frias, B. Aarup, Durability of ultra-high strength concrete: Compact reinforced composite, BHP96 Fourth International Symposium on Utilisation on High Strength/High Performance Concrete Paris, France, 1996, pp. 529-534.
- [8] N. Roux, C. Andrade, M. Sanjuan, Experimental study of durability of reactive powder concretes, Journal of Materials in Civil Engineering, 8 (1996) 1-6.

- [9] G. Orange, J. Dugat, P. Acker, Ductal®: New ultra high performance concretes. Damage resistance and micromechanical analysis, Fifth International RILEM Symposium on Fibre-Reinforced Concrete (FRC), 2000, pp. 781-790.
- [10] P. Rossi, Ultra-high performance fibre reinforced concretes (UHPFRC): an overview, In Proceeding Fifth RILEM Symposium on Fibre-Reinforced Concretes (FRC) - BEFIB' 2000, 2000, pp. 87-100.
- [11] B. Aarup, CRC–Applications of fibre reinforced high performance concrete, Concrete Plant International CPI, (2007) 1-10.
- [12] D.K. Harris, C.L. Roberts-Wollmann, Characterization of punching shear capacity of thin ultra-high performance concrete slabs, Proceedings of the International Symposium on Ultra High Performance Concrete, Kassel University Press GmbH, Kassel, Germany, 2008, pp. 727-734.
- [13] C. Joh, H. Hwang, E. Choi, J.J. Park, B.-S. Kim, Punching shear strength estimation of UHPC slabs, Proceedings of the International Symposium on Ultra High Performance Concrete, Kassel University Press GmbH, Kassel, Germany, 2008, pp. 719-726.
- [14] L. Moreillon, J. Nseir, R. Suter, Shear and flexural strength of thin UHPC slabs, Proceedings of Hipermat 2012, 3rd International Symposium on UHPC and Nanotechnology for High Performance Construction Materials, Kassel University Press GmbH, Kassel, Germany, 2012, pp. 748-756.
- [15] T. Le, Ultra high performance fibre reinforced concrete paving flags, University of Liverpool, Liverpool, United Kingdom, 2008, pp. 387.
- [16] A.M. Neville, Properties of concrete, Prentice Hall, 5th Edition 2012.

[17] BS EN 1992-1-1, Eurocode 2: Design of concrete structures-Part 1-1: General rules and rules for buildings, British Standards Institution, 2004, pp. 230.

[18] U.S. Geological Survey, Loma Prieta, California Earthquake: [http://gallery.usgs.gov/sets/1989 Loma Prieta, California Earthquake/list/_/5](http://gallery.usgs.gov/sets/1989_Loma_Prieta,_California_Earthquake/list/_/5), 1989.

[19] Portland cement association, Innovative concrete bridge wins quality initiative structure award- <http://www.cement.org/exec2/05-04-09.htm>.

[20] Park H, Ulm F-J, Chuang E, Model-based optimization of ultra high performance concrete highway bridge girders, Massachusetts Institute of Technology, Boston, USA, 2003, pp. 139.

List of Figures



Figure 1: Failure of the Struve Slough Bridge due to Loma Prieta Earthquake, USA [18].

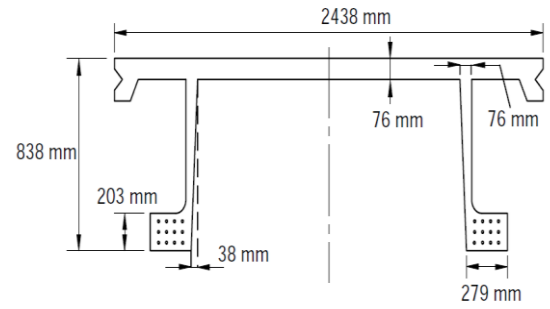


Figure 2: Optimised UHPC bridge girder design [19, 20].

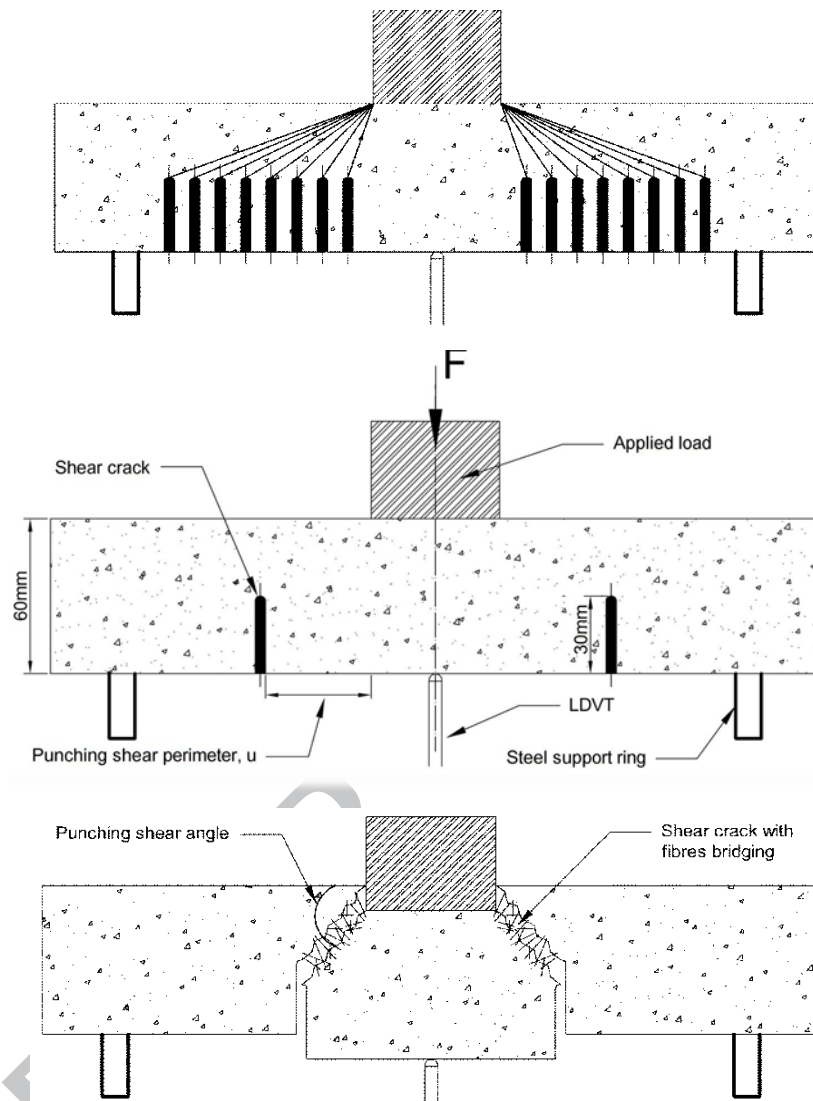


Figure 3: Indicative diagram of test setup.

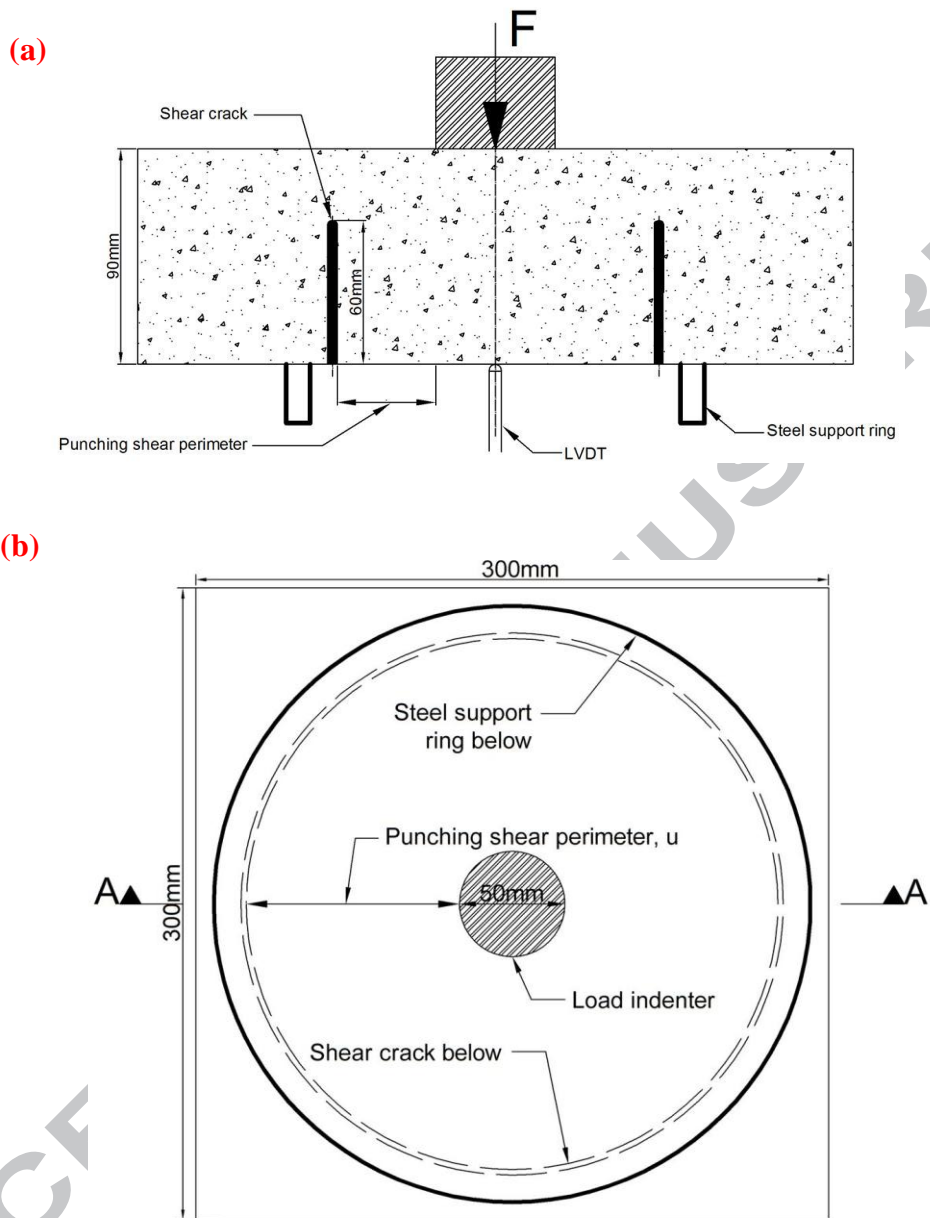


Figure 4: The final test setup: (a) Section view, and (b) Plan view.



Figure 5: Specimen before and after grinding



Figure 6: Specimen preparation, shear notch inducers using diamond drills

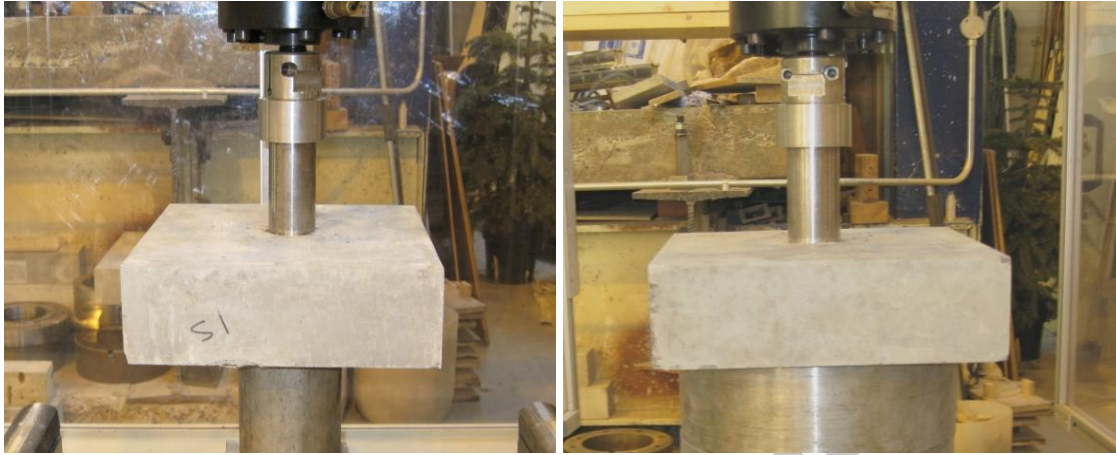


Figure 7: Test setup in the testing rig.

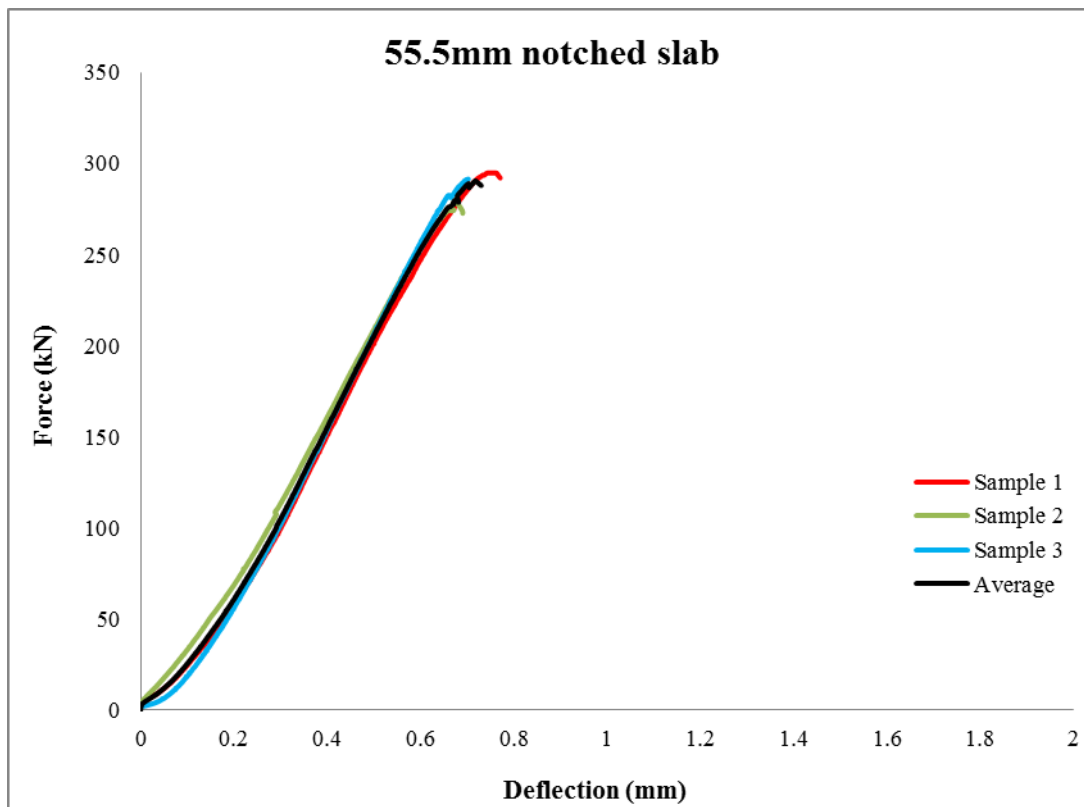


Figure 8: Punching shear load versus vertical deflection for specimens with a punching shear perimeter distance equal to $0.09d$ (55.5 mm notch perimeter).

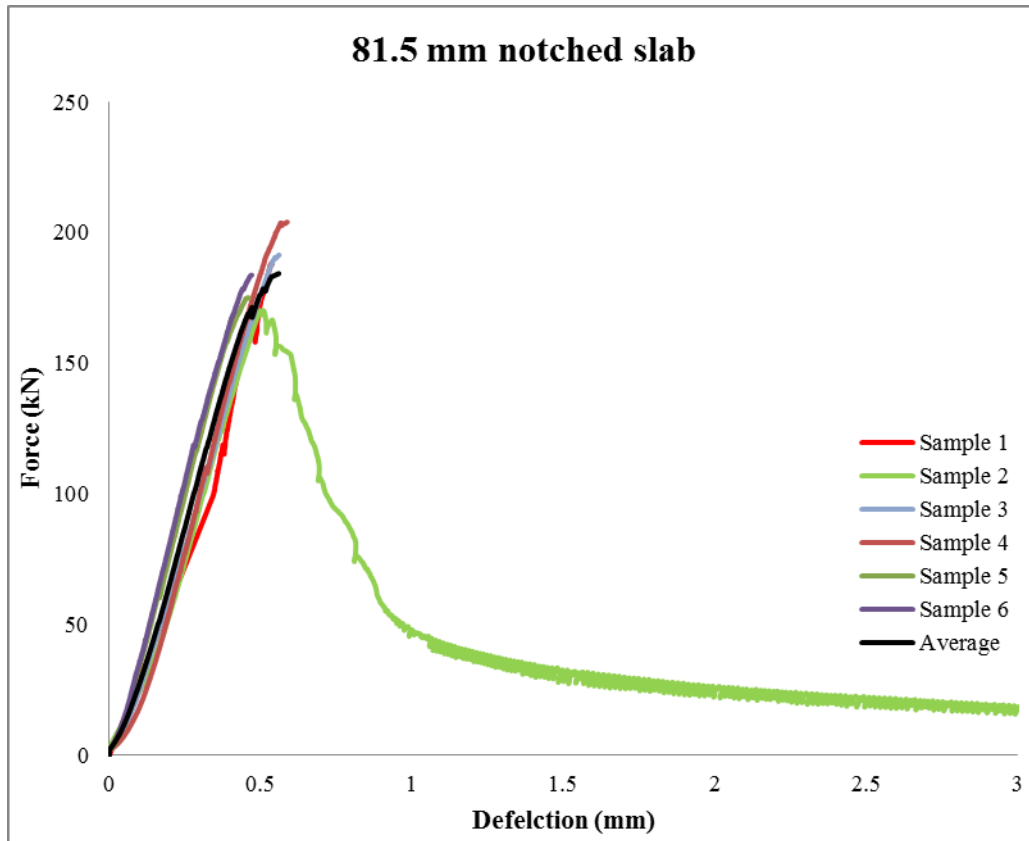


Figure 9: Punching shear load versus vertical deflection for specimens with a punching shear perimeter distance equal to $0.53d$ (81.5 mm notch perimeter).

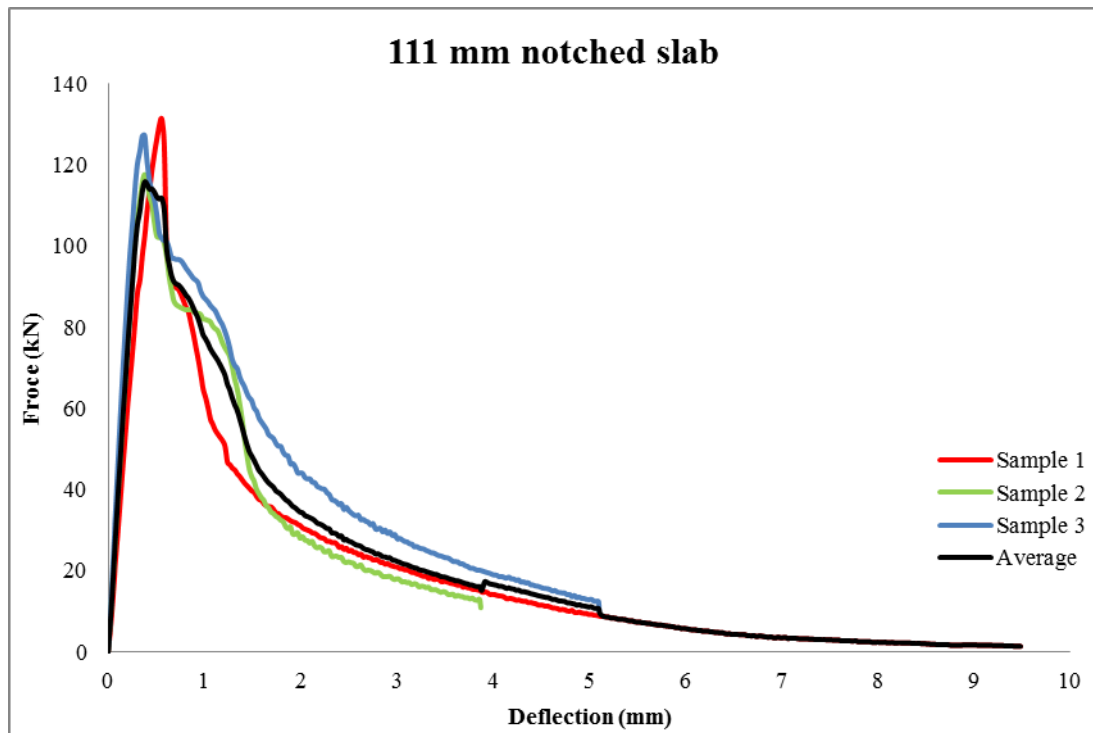


Figure 10: Punching shear load versus vertical deflection for specimens with a punching shear perimeter distance equal to $1.02d$ (111 mm notch perimeter).

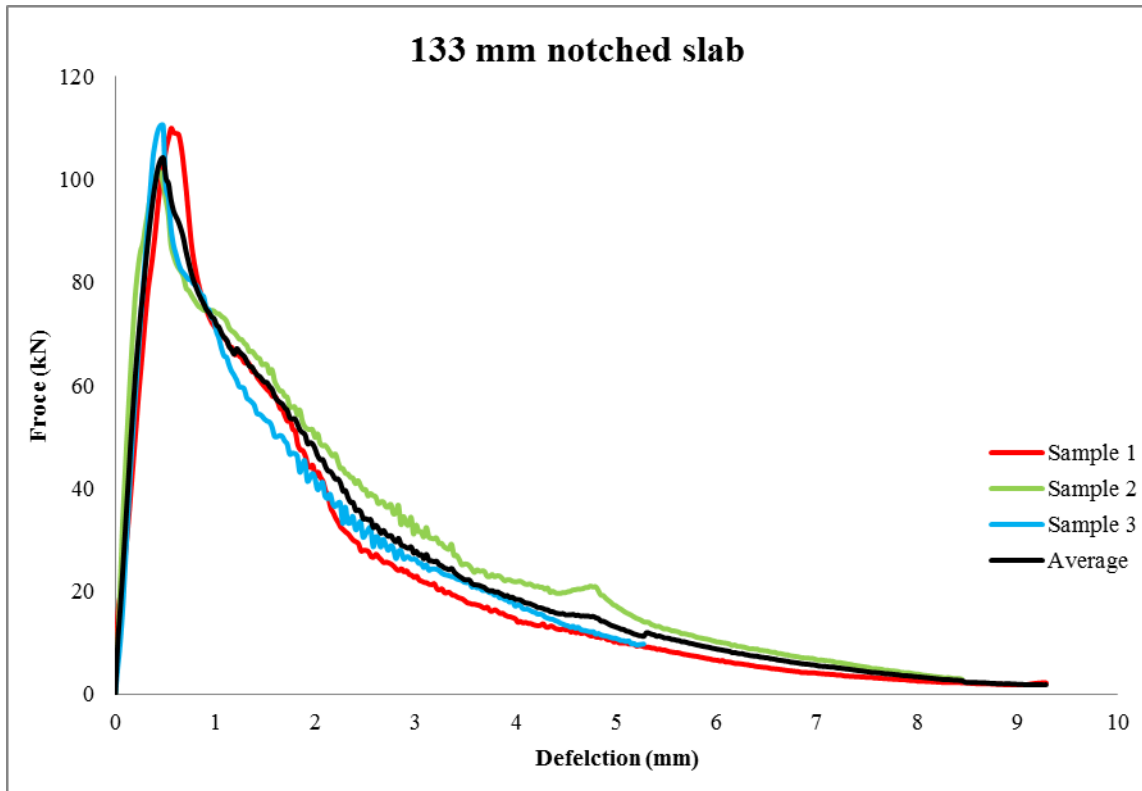


Figure 11: Punching shear load versus vertical deflection for specimens with a punching shear perimeter distance equal to $1.38d$ (133 mm notch perimeter).

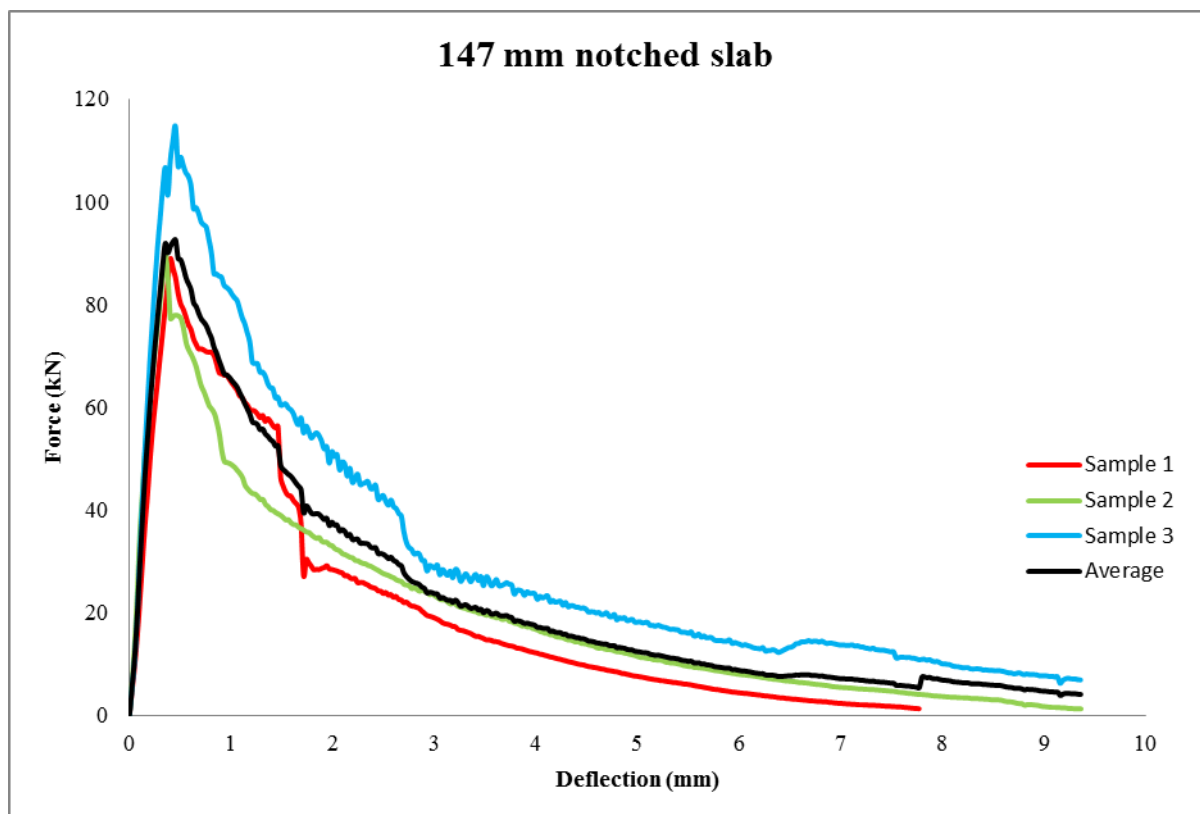


Figure12: Punching shear load versus vertical deflection for specimens with a punching shear perimeter distance equal to $1.62d$ (147 mm notch perimeter).

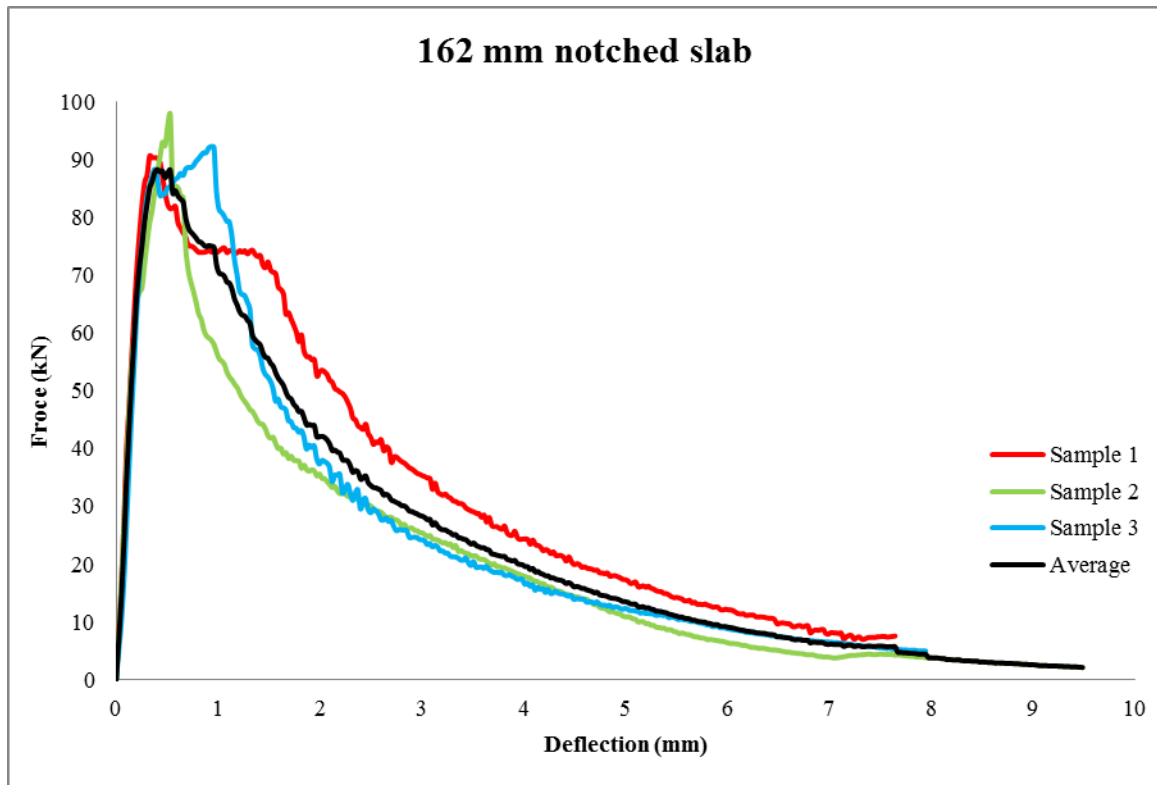


Figure13: Punching shear load versus vertical deflection for specimens with a punching shear perimeter distance equal to $1.87d$ (162 mm notch perimeter).

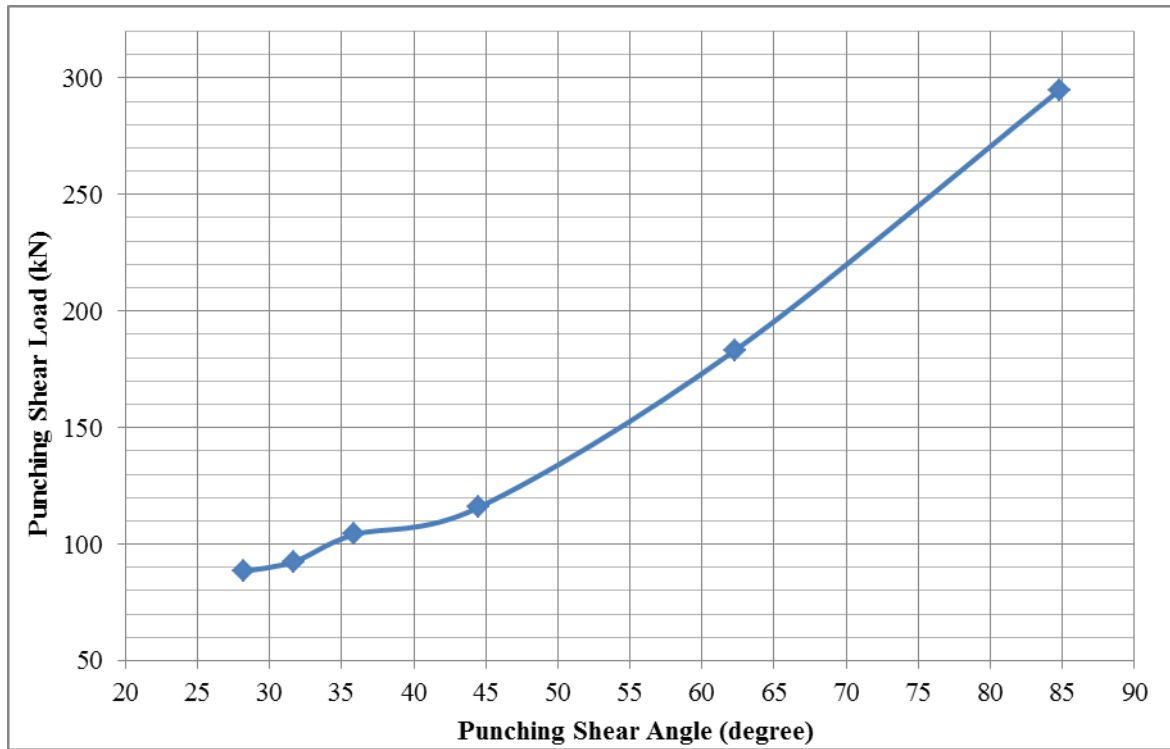


Figure 14: Punching shear angle versus punching shear load.

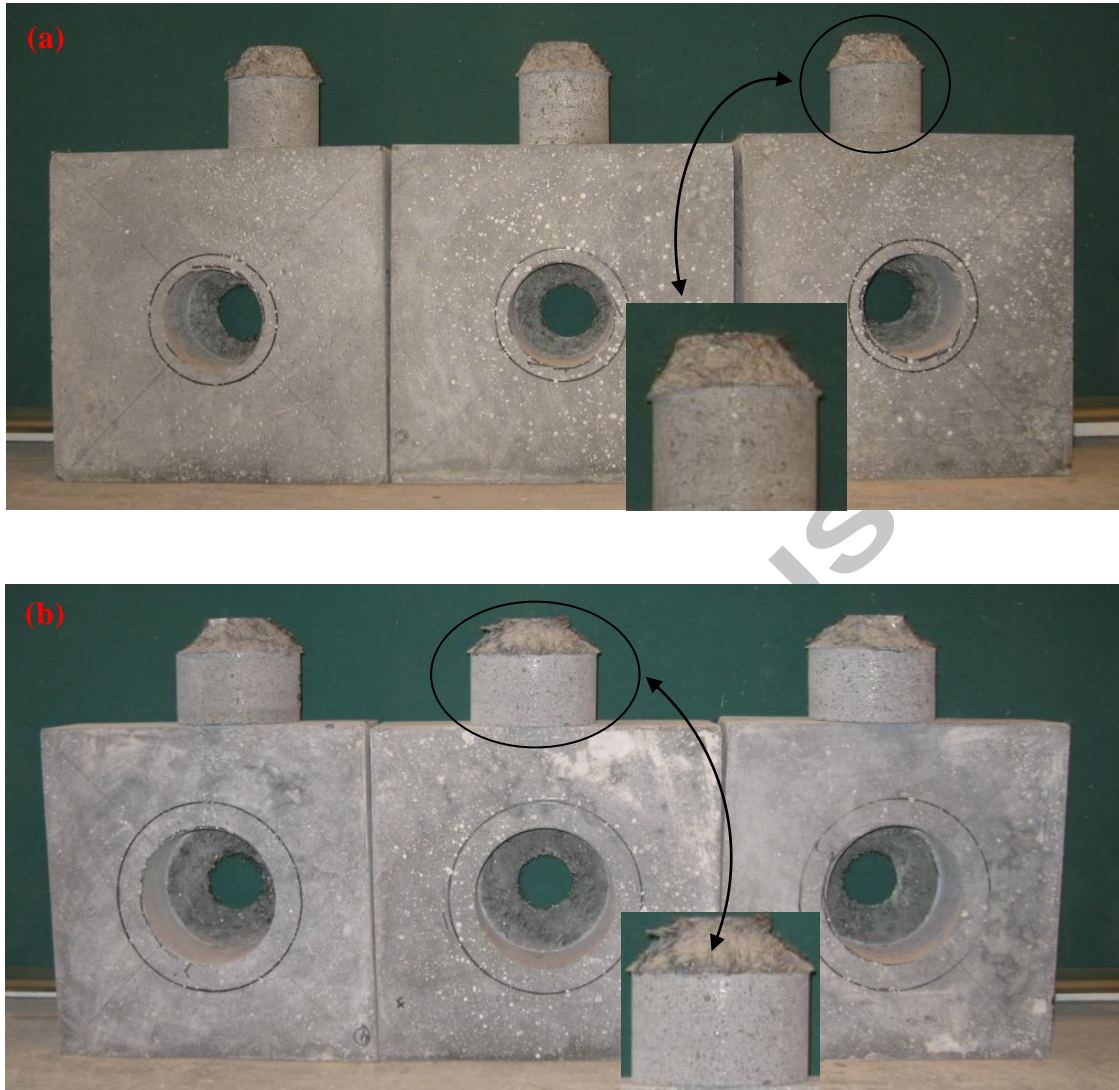


Figure 15: The punching shear failure modes for: (a) The 0.09d specimens, and (b) The 0.53d specimens.

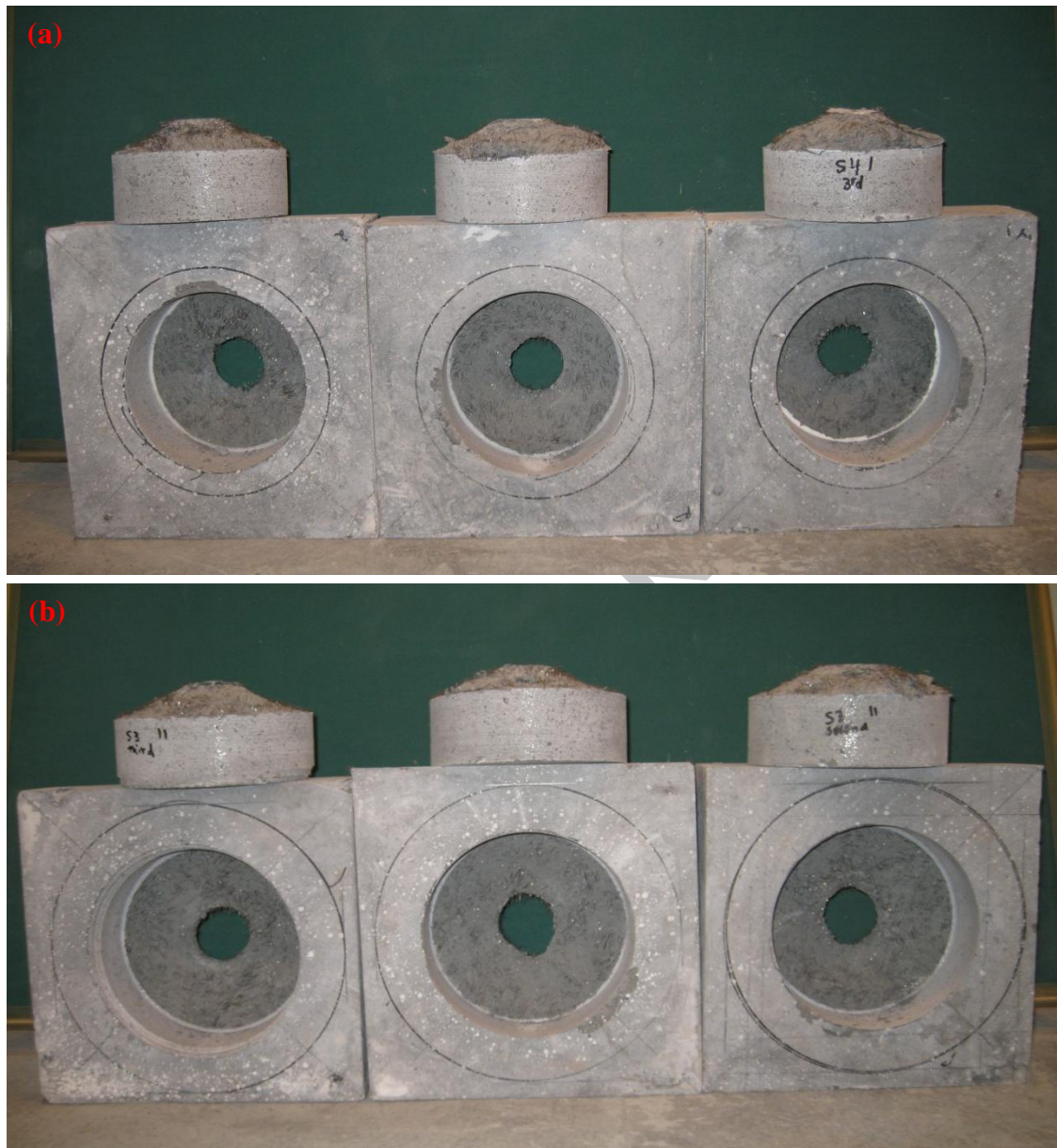


Figure 16: Typical punching shear failure mode for: (a) 1.62d, and (b) 1.87d.



Figure 17: Typical failure on the loading side.

List of Tables

Table 1: Mix design for UHPFRC.

Material	(kg/m ³)
Cement (CEM1: 52.5N)	657
GGBS	418
Silica fume	119
Silica sand (average size 0.27 mm)	1051
Superplasticisers	40
Water	185
Steel fibre (2% volume)	157

Table 2: Summary of slab specimens and support arrangements in the third phase

Notch diameter (mm)	Support, inside-diameter (mm)	Support thickness (mm)	Basic control perimeter	Punching shear angle (degree)
55.5	60	8	0.09d	84.8
81.5	98	8	0.53d	62.3
111	143	12.5	1.02d	44.5
133	150	8	1.38d	35.9
147	173	10	1.62d	31.7
162	194	12.5	1.87d	28.2

Table 3: Phase three test results.

Notch diameter (mm)	u	θ (degrees)	V_{rd} (kN)	δ_{rd} (mm)	Failure mode
55.5	0.09d	84.8	294.86	0.762	Brittle
81.5	0.53d	62.3	183.26	0.561	Brittle ¹
111	1.02d	44.5	115.79	0.379	Ductile
133	1.38d	35.9	104.18	0.479	Ductile
147	1.62d	31.7	92.58	0.453	Ductile
162	1.87d	28.2	88.27	0.405	Ductile

¹ Out of six specimens, five brittle and one ductile failure was reported.